Charge collection in silicon p^+-n-n^+ -structures at temperature 40 mK

© E.M. Verbitskaya¹, I.V. Eremin¹, N.N. Fadeeva¹, V.K. Eremin¹, V.O. Zbrozhek², A.A. Yablokov², I.D. Isakov^{1,3}

603155 Nizhny Novgorod, Russia

³ St. Petersburg Electrotechnical University "LETI",

197022 St. Petersburg, Russia

E-mail: elena.verbitskaya@mail.ioffe.ru

Received June 11, 2025 Revised June 20, 2025 Accepted June 20, 2025

Charge collection in 1 mm thick Si p^+-n-n^+ -structures in the range of electric field up to ~ 7.5 kV/cm is studied at a temperature 40 mK, which is the target temperature for the operation of Si bolometric antineutrino detectors. Analysis of the structure current responses shows that under these conditions the silicon bulk is transformed into an electrically neutral insulator with a trapping time of nonequilibrium electrons of ~ 370 ns and holes of more than 1 μ s. Charge collection demonstrates two stages: a space charge limited current and a drift of a thin carrier package with kinetics controlled by the collected charge magnitude. Calculations of the change in the electric field accompanying the drift are presented and a decrease in the carrier collection time to 10 ns is shown.

Keywords: silicon p^+-n-n^+ -structure, current response, electric field, nonequilibrium carriers, collection time, antineutrino.

DOI: 10.61011/SC.2025.03.61563.8123

1. Introduction

The use of semiconductor devices at temperatures T of hundredths of a degree Kelvin was formed in connection with the task of searching for Weakly Interacting Massive Particles (WIMPs) as possible candidates responsible for the existence of dark matter in the Universe. search experiments are being developed by the Cryogenic Dark Matter Search (CDMS) [1,2] and Edelweiss [3] collaborations using germanium and silicon bolometric detectors at temperatures in the tens of millikelvins (mK): with a planned future mass of tens of kilograms and sensitivity better than 1 keV. In such detectors, it is assumed that it is not the electrical response of the detector that is measured, but rather the thermal response, i.e., the pulsed increase in temperature of the detector's sensitive elements (SE) due to the energy released in them by a particle. At the same time, fundamental fluctuations in the signal do not occur during the energy division between the ionization loss channel, i.e., the generation of nonequilibrium electrons and holes, and phonon formation losses. Achieving a low noise level is ensured by using transient-edge sensors (TES) with signal detection by a "superconducting quantum interference device" (SQUID) type amplifier. Another area of semiconductor detectors application is research in the field of neutrino physics. For instance, a 1.5 kg detector based on HP (High purity) Ge was built in the GEMMA project [4] to study the magnetic moment of reactor antineutrinos. Within the framework of

the scientific program of the National Center for Physics and Mathematics (NCFM), Sarov, section 8 "Hydrogen isotope physics" [5], an experiment is currently being prepared to study the magnetic moment of an electron antineutrino with a tritium source using the reaction [6]:

$${}_{1}^{3}\mathrm{H} \rightarrow {}_{2}^{3}He + e^{-} + \overline{\nu}_{e}, \tag{1}$$

and three types of detectors, including silicon (Si) bolometric detectors with a total weight of up to $10\,\mathrm{kg}$ with an operating temperature T in the range of $10-50\,\mathrm{mK}$ and a target detection threshold of few eV. To ensure the necessary sensitivity, it is planned to implement an internal amplification of the thermal signal in the SE [7] due to the Joule–Lenz effect, i.e., the release of heat during the movement of charge carriers in a solid under the influence of an electric field. The additional energy ΔE in such SE, formed due to the drift of nonequilibrium charge carriers (NCC) created by the detected particle (in this case, an antineutrino), is expressed in the one-dimensional model as

$$\Delta E = \int_{0}^{\eta} Q_e(x,t)F(x,t)dx + \int_{\eta}^{d} Q_h(x,t)F(x,t)dx, \quad (2)$$

where $Q_{e,h}$ is the charge of electrons or holes formed by a particle that drifts at a point with the coordinate x, F(x,t) is the electric field, depending on the coordinate x normal to the surface of the structure, and time t, η is the coordinate of the particle registration point where the NCC is generated,

¹ loffe Institute,

¹⁹⁴⁰²¹ St. Petersburg, Russia

² Alekseev State Technical University,

and d is the thickness of the SE. If the trapping time constant of nonequilibrium carriers τ_{tr} is much longer than their collection time t_{col} , the value of Q is constant. In this case, a set of drift trajectories of packages of electrons and holes connects the electrodes, between which there is a potential difference corresponding to the applied voltage V, which determines the independence of the allocated additional energy from η , i.e. $\Delta E = QV$. When τ_{tr} and t_{col} are commensurate, it becomes smaller and is determined by the transport parameters of electrons and holes and their lifetimes. For bolometric detectors developed in the program No. 8, the thickness of the sensitive area of which will be several centimeters, and $T = 10-50 \,\mathrm{mK}$, the ratio $t_{\rm col}/\tau_{tr}$ may be critical. This is due to the fact that both deep impurity centers and shallow donors and acceptors (phosphorus and boron, respectively), whose concentration in high resistivity Si at room temperature is $(3-7) \cdot 10^{11}$ cm⁻³, can affect the efficiency of NCC capture in silicon.

The characteristics of Si detectors under deep cooling were actively studied earlier in connection with their development for experiments at the Large Hadron Collider (LHC) [8,9] and were carried out at a temperature of superfluid helium (1.9 K). This was due to the task of monitoring the intensity of the radiation field in the region of the LHC's superconducting magnets, but the research focused on the degradation of the detector signal under the influence of relativistic protons due to the drop of τ_{tr} .

The purpose of this paper is an experimental study of the kinetics of charge collection in silicon detector p^+-n-n^+ -structures at T in tens of millikelvins, related to the antineutrino detectors developed in the Program N^0 8 with internal thermal signal amplification, charge drift in which occurs at electric field ranging from hundreds of V/cm to units of kV/cm. The experimental data presented in this paper were obtained by measuring the pulse current response of Si structures in a closed-loop dilution cryostat at $T=40\,\mathrm{mK}$ and continue the studies presented earlier in Ref. [10].

2. Experimental samples and current response measurement techniques

The experiments used detector p^+-n-n^+ structures made on n-Si wafers with a thickness of 1 mm with an orientation of $\langle 100 \rangle$ and a resistivity of $7 \, \text{kOhm} \cdot \text{cm}$ (corresponds to the concentration of donors $N_0 \approx 6 \cdot 10^{11} \, \text{cm}^{-3}$). The area of the contact p^+ -layer obtained by boron implantation was $10 \times 10 \, \text{mm}^2$; the contact was surrounded by a structure of four p^+ -rings optimized for stabilizing current-voltage curves at room temperature. Phosphorus atoms were implanted to create a rear contact n^+ -layer on the entire surface of the chip measuring $13 \times 13 \, \text{mm}^2$. The concentration of boron and phosphorus atoms in the p^+ -and n^+ -layers was $\geq 10^{18} \, \text{cm}^{-3}$, which was sufficient for silicon degeneration at room temperature. Metallization of the contact layers with aluminum had optical windows with

an area of $\sim 1 \, \text{mm}^2$, which was necessary for generating electron-hole (e-h) pairs with a laser and measuring the current response of the structures.

Measurements of the current response of the samples were carried out at Nizhny Novgorod State Technical University at $T = 40 \,\mathrm{mK}$. The experimental setup based on a closed-loop dilution cryostat and the measurement procedure are described in detail in Ref. [10]. cooling time of the cold flange of the cryostat from room temperature ($\sim 20^{\circ}$ C) to the target temperature was ~ 20 h. The current responses of the p^+-n-n^+ structures were obtained by generating the NCC with a pulsed laser with a wavelength of 670 nm and a pulse duration of 47 ps. The diameter of the laser light spot on the sample surface was $\sim 2 \, \text{mm}$. However, due to problems with adjusting the position of the fiber-optic cable in relation to the optical windows on the contacts and the radial intensity profile in the beam, the concentration of e-h-pairs in the contact areas was different, which was further enhanced by the difference in the doping profile of p^+ and n^+ -layers.

The current responses were recorded by a digital oscilloscope with an analog band of 2 GHz and an input impedance of 50 Ohm. The signal output lines from the samples located on the cold flange of the cryostat to the oscilloscope included a system of cryogenic coaxial cables with a total length of $\sim 2\,\mathrm{m}$ inside the cryostat and external high-frequency coaxial cables up to 5 m long.

3. Experimental results of pulse current response of silicon p^+ -n- n^+ structures at 40 mK

Measurements of the pulse current response of the p^+ -n- n^+ -structure were performed at a reverse voltage and irradiation of one side of the sample with a pulsed laser. A negative voltage was applied to the p^+ -contact from which the signal was recorded, while the n^+ -contact was grounded. During the time required to set the required voltage on the structure, laser pulse irradiation was interrupted to minimize heating of the samples. Measurements at constant voltage and different relaxation times of the samples between laser pulse applications showed the identity of the results, which indicates the stability of the temperature necessary for the reliability of the data. The depth δ of NCC generation near the contacts at $T = 40 \,\mathrm{mK}$ was $\sim 10 \,\mu\mathrm{m}$ [9], which made it possible to consider the process of charge collection as the drift of a flat carrier package in a one-dimensional geometry. In this case, the resulting drift current i when the charge qmoves at the coordinate x at the time t is described by the Shockley—Ramo expression [11]:

$$i(x) = qF_w(x)\mu(F, T)F(x), \tag{3}$$

where μ is the mobility of the drifting carriers, depending on F and T and F_w is the weighting electric field, which determines the efficiency of charge induction on the contacts, and in plane-parallel geometry is 1/d.

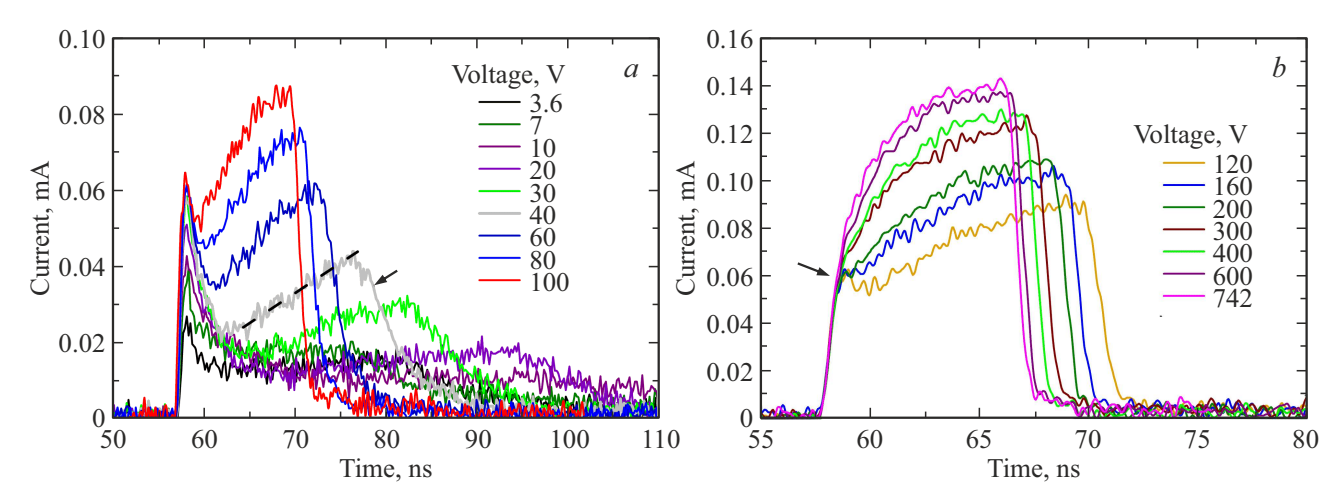


Figure 1. Current responses of Si p^+-n-n^+ -structure during electron drift at voltage: $a-\le 100 \,\mathrm{V},\, b-\ge 120 \,\mathrm{V}.$

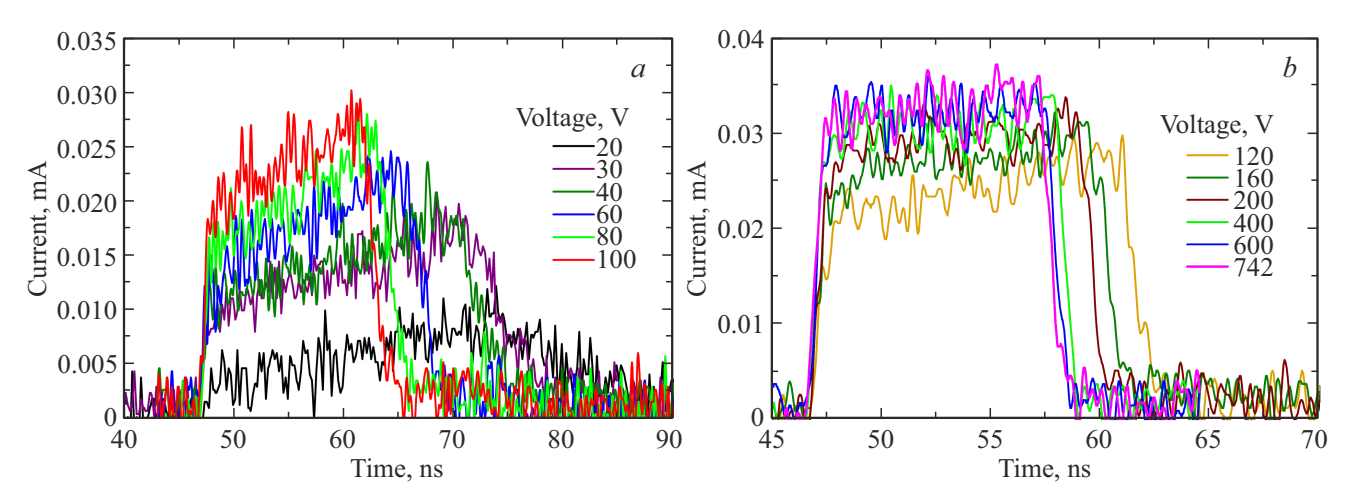


Figure 2. Current responses of Si p^+-n-n^+ -structure with hole drift at voltage: $a-\le 100\,\mathrm{V},\,b-\ge 120\,\mathrm{V}$.

Figures 1 and 2 show the pulse current responses of the sample when generating e-h-pairs at each of the contacts in the range of $V=5-742\,\mathrm{V}$, obtained in a series of measurements with ~ 30 values of V. It should be noted that the scales on the axes differ for a detailed visualization of the responses. Figure 1 shows examples of typical waveforms when a p^+ -contact is irradiated with a laser and, accordingly, determined by the electron drift to the n^+ -contact. The following characteristic elements of their shape can be distinguished in a series of pulses.

- At voltages of $3.6-100\,\mathrm{V}$ (Figure 1,a), a peak is observed near the pulse leading edge, which can be interpreted as the efflux of carriers from the package of e-h-pairs generated by a laser pulse, with simultaneous electron drift to the n^+ -contact and holes to the p^+ -contact; the latter is clearly visible in the total current.
- The peak is followed by a close-to-linear region of current growth (approximation is shown by a dashed line for $V=40\,\mathrm{V}$), ending with a maximum turning into a slow decline (indicated by the arrow).

- As the voltage increases, the slope of linear region grows, and the beginning of the current drop becomes a well-defined point, the time to reach which decreases with increasing voltage. At the same time, the peak remains at the beginning of the pulse, decreasing in duration.
- The peak practically disappears at $V > 100 \,\mathrm{V}$, and the shape of the signal top with a further increase of V is characterized by a progressive rise in current with a tendency to slow down its growth rate (Figure 1, b).
- The voltage range of $120-742\,\mathrm{V}$ is characterized by the absence of a slow decay region and the resulting sharp drop in the signal, the duration of which is constant and close to the rise time of the current response front.

The current responses shown in Figure 1, b highlight the moment of fracture of its front (shown by the arrow), when its fast component turns into a slow one, where the current continues to increase, but at a decreasing rate. The fast component of the response front has a rise time $t_r \sim 0.7 \, \mathrm{ns}$, which is close to the time resolution of the signal recording path, including the oscilloscope response time $\tau_{\rm osc} < 0.5 \, \mathrm{ns}$

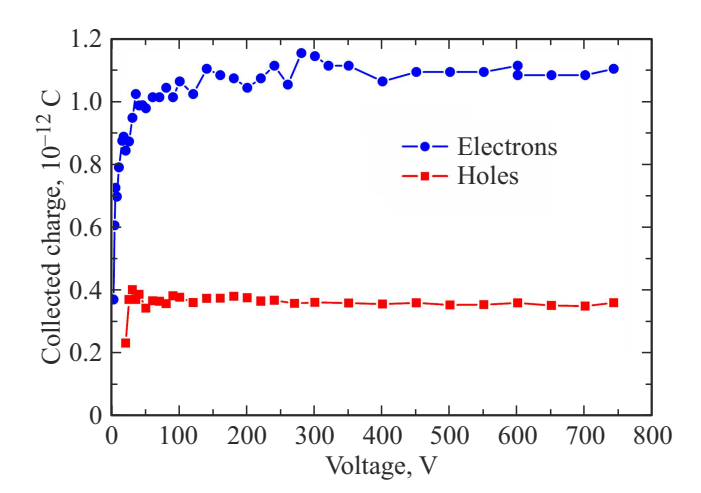


Figure 3. Voltage dependences of the collected charge of electrons and holes for Si p^+ –n– n^+ -structure.

and the sample response time constant $\tau_{\rm smp} = R_{\rm osc} \cdot C_{\rm smp}$, where $R_{\rm osc}$ is the input impedance of the oscilloscope and $C_{\rm smp}$ is the sample capacitance in the holder, equal respectively to 50 Ohm and 8 pF, which gives $\tau_{\rm smp} = 0.4$ ns. At $V \ge 400$ V, the current response decay time has a similar value, $t_d \approx 0.6$ ns.

The results for the voltage range of $V > 100\,\mathrm{V}$ allow concluding that the process of charge collection is associated with the drift of a thin package of electrons with a thickness δ to the n^+ -contact, which, upon reaching contact, leaves the drift region within the time of $< 0.6\,\mathrm{ns}$. Due to the small thickness of the drifting layer, an increase in the current at the top of the pulses, defined by expression (3), can only be associated with an increase in the electric field.

Figure 2 shows the current responses of the sample when the n^+ -contact is irradiated with a laser and, accordingly, holes drift towards the p^+ -contact. These responses have the following specific features in comparison with the pulses in Figure 1.

- There is no peak near the pulse leading edge that could visualize the electron drift to the p^+ -contact (Figure 2, a).
- The responses show a linear increase in current over time at $V \leq 100\,\mathrm{V}$, to a maximum value followed by a decrease, which becomes sharp already at $V \approx 40\,\mathrm{V}$.
- The most significant difference between the responses during hole drift is that at $V \ge 400 \,\mathrm{V}$ the maximum current and duration of the responses slightly change, and the tops of the pulses are almost flat (Figure 2, b).

The most likely reason for most of the differences in the series of signals shown in Figure 2 is the lower number of generated e-h-pairs near the n^+ -contact than in the series of pulses shown in Figure 1. As can be seen from the dependences of the collected charge $Q_{\rm col}$ on voltage, the absolute values $Q_{\rm col}$, determined by integrating current responses in the range of $t_{\rm col}$, reach saturation at 100 and 25 V in the case of electron and hole drift, and amount to $1.1 \cdot 10^{-12}$ and $3.6 \cdot 10^{-13}$ C (Figure 3).

The paradox is the increase in current over time for pulses from both electrons and holes, which was observed earlier in Ref. [10] when exposed to a laser with a wavelength of 670 nm. Interpretation of this fact, according to expression (3), leads to the conclusion that μF increases in time when both electrons and holes are collected, i.e., in case of electron drift, the steady-state electric field in the sample increases from p^+ - to n^+ -contact, and vice versa, when holes drift, the electric field at the p^+ -contact is higher than at the n^+ -contact, which is impossible. Thus, study of experimental signals generated in p^+-n-n^+ -structures in the range from room temperatures up to 6 K [12], showed that the gradient di/dt at the top of current pulses generated by electron transfer at each temperature is negative, while in the pulses for hole drift at the same temperatures it is positive, as would be expected for a constant negative gradient of electric field.

The explanation of the observed paradox is given in section 4.2.

4. Discussion of the results

4.1. Capture of nonequilibrium charge carriers

To solve the study problem, i.e., to obtain data on the time of collection of a nonequilibrium charge in the p^+-n-n^+ -structure at 40 mK, it was assumed that $t_{\rm col}$ is equal to the time difference between the level of 0.5 of the amplitude of the decay and the leading edge of the signal. This made it possible to formalize the processing of the results and minimize the influence of the waveform on the determination of the NCC collection time as a value affecting charge loss due to carrier trapping at the levels of impurity atoms. The obtained dependences of the electron and hole collection time on the mean electric field $F_{\text{mean}} = V/d$ are shown in Figure 4, a. The dependences have 2 regions: a rapid t_{col} decay in the range of tens ns at $F < 1 \,\text{kV/cm}$ and its slow decrease at higher F_{mean} up to a minimum, where the collection times of electrons and holes are 9 and 11 ns, respectively. It should be noted that the nature of $t_{\rm col}(F_{\rm mean})$ -dependencies correlates with the change in the value of the collected charge depending on the voltage, which is shown in Figure 4, b as the dependence of the normalized charge $Q_{\text{col},n}$ on F_{mean} . A sharp decay of the collection time occurs in almost the same voltage range as the rise of the collected charge. Combining the data in Figure 4, a and b is shown in Figure 5, where τ_{col} are given on According to the dependence of a logarithmic scale. Q_{col_n} on t_{col} related to the capture of charge carriers when they are collected in structures with plane-parallel contacts [13]

$$Q_{\text{col},n} \sim \exp\left(-\frac{t_{\text{col}}}{\tau_{tr}}\right),$$
 (4)

The experimental data for electrons can be approximated by a line (Figure 5), the slope of which gives $\tau_{tr} = 380$ ns.

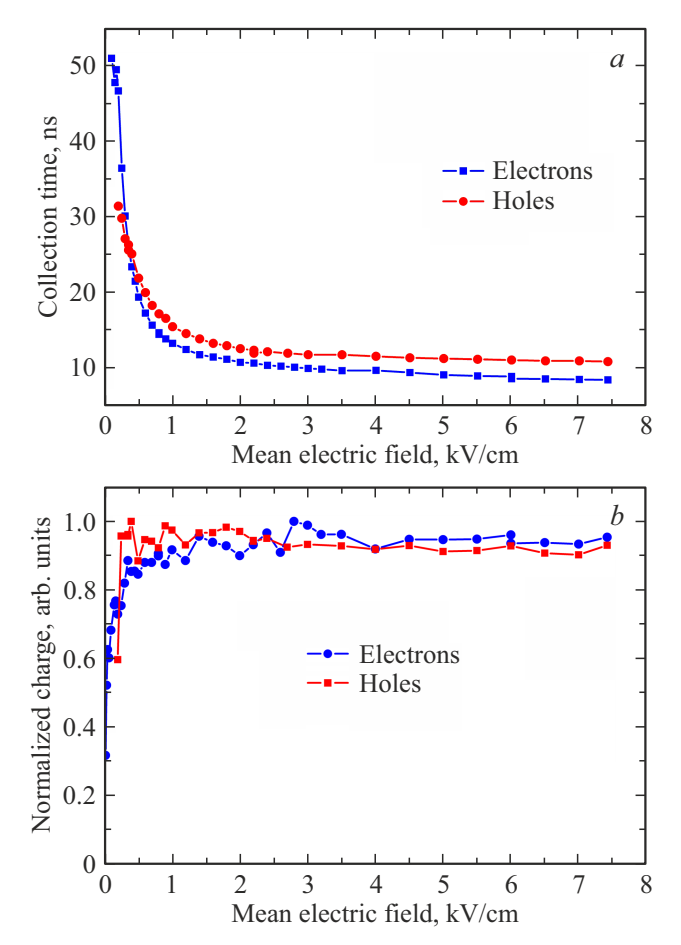


Figure 4. The dependences of the time of carrier collection (a) and the normalized charge (b) on the mean electric field in the Si p^+-n-n^+ -structure.

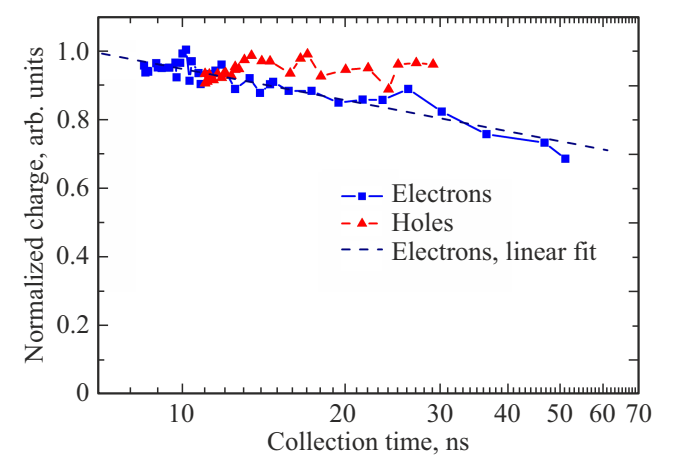


Figure 5. The dependence of the normalized collected charge on the collection time during the drift of electrons and holes.

Since the approximation corresponds to the entire voltage range, the resulting value τ_{tr} applies both to electron losses in the cloud of e-h-pairs created by a laser pulse near the p^+ -contact and in a package of drifting electrons. The

collected charge for holes is practically independent of $t_{\rm col}$ in the range of $F=(0.2-7.45)\,\rm kV/cm$ (Figure 5), which implies that the trapping time of nonequilibrium holes lies at least in the range of μ sec.

A significant difference in the trapping times of electrons and holes in pure high-resistivity silicon at $T=40\,\mathrm{mK}$ indicates 2 facts.

- The value of $\tau_{tr_e} \approx 380\,\mathrm{ns}$ at $40\,\mathrm{mK}$ should be attributed to the capture of electrons at the energy levels of shallow impurities, since at room temperature τ_{tr} of carriers, determined by impurities and defects creating deep levels, is tens of $\mu\mathrm{sec}$.
- Electrons are captured at the levels of phosphorus atoms, the concentration of which exceeds the concentration of shallow acceptors (boron atoms) by several times.

The result shows the importance of using the purest silicon for bolometric detectors across the entire spectrum of electrically active impurities and defects. In addition, the large difference in the trapping times of electrons and holes indicates the dependence of the amplitude of the thermal signal of the bolometric detector on η during its operation in the internal thermal amplification mode. Indeed, in a detector with a uniform electric field in the sensitive region, the potential linearly depends on the coordinate x as V(x) = Fx (x = 0 at the p^+ -contact). When the particle is detected at the point $x = \eta$, the potential differences ΔV traversed by holes and electrons until they reach the corresponding contacts are equal to $\Delta V_h = F \eta$ and $\Delta V_e = F(d - \eta)$ and are different. In this case, the hole component $\Delta E_h = Q_h \Delta V_h$ of the thermal signal does not depend on the time of hole collection, whereas the electronic component $\Delta E_e = Q_e \Delta V_e$ due to the dependence of Q_e on t_{col_e} will lead to the influence of η on ΔE , which will degrade the energy resolution of the detector.

4.2. Mechanisms of NCC collection

The paradox noted above in the top slope of the current responses of the silicon $p^+ - n - n^+$ -structure requires separate consideration. Pulse signals make it possible to distinguish two types of responses with different carrier collection kinetics and their corresponding processes. The first one includes responses from electrons at $V \leq 100\,\mathrm{V}$, for which a time-extended current drop region is observed (Figure 1, a), which can be interpreted as collecting the charge from a package of electrons and holes in the mode of space-charge-limited current (SCLC) [14,15]. This process develops when a source is formed near the p^+ -contact, providing a long-term supply of nonequilibrium electrons to the drift region.

The second type of pulses, characteristic of the kinetics of electron collection in the range of $V > 100 \, \mathrm{V}$ (at $V > 40 \, \mathrm{V}$ for holes), does not have regions of prolonged current drop, which indicates a change in the mechanism of their collection. A special feature is the increase of the current over time, which, according to expression (3), indicates a progressive increase of the drift velocity μF in the package.

It can only occur due to an increase of the electric field in the drift region as the electron package approaches the n^+ -contact. As it was experimentally established earlier, phonon-stimulated carrier tunneling in the Poole–Frenkel effect, which promotes ionization of shallow energy levels of phosphorus atoms in case of cooling [12] does not work at temperatures below 800 mK [10]. As a result, the freezing of the equilibrium filling of impurity centers at $T=40\,\mathrm{mK}$, including shallow impurities, in the absence of free carriers n=p=0 guarantees a stationary effective (difference) concentration of spatial charge N_{eff} close to zero, and silicon at temperatures below 800 mK is an electrically neutral insulator even at F of the order of few kV/cm.

Under these conditions, the presence of a drifting package in the p^+ -n- n^+ -structure leads to a significant disturbance of the electric field profile in the volume, consisting in the occurrence of a voltage jump ΔF at the location of the carrier package. According to the Poisson equation in the 1D model, with a uniform electron concentration n in the package, the jump value is defined as

$$abs(\Delta F) = \frac{en\delta}{\varepsilon \varepsilon_0} = \frac{Q_s}{\varepsilon \varepsilon_0},\tag{5}$$

where e is the elementary charge, ε and ε_0 are the dielectric constants of silicon and vacuum, respectively, and Q_s is the surface charge density in the package. For the front and rear of the drifting package, the field F_f and F_r , respectively, should be different and, subject to the constancy of the voltage applied to the structure, are determined by the relations:

$$F_f = \frac{V}{d} + \frac{en\delta x_f}{\varepsilon \varepsilon_0 d},\tag{6}$$

$$F_r = \frac{V}{d} + \frac{en\delta}{\varepsilon \varepsilon_0} \left(\frac{x_r}{d} - 1 \right). \tag{7}$$

An illustration of the distribution of F for the three positions of the package in a structure with a thickness of 1 mm and the parameters defined by the expressions (5)-(7) is qualitatively presented in Figure 6.

The ratio $F_f > F_r$ is characteristic, which, as the drift proceeds, leads to an increase in package thickness and a change in distribution n(x). The current $i = qF_w\mu F$, which occurs during package drift and consists of currents induced on the contacts by each individual charge, can be defined as the displacement of the package centroid with the electric field F_c and a coordinate x_c . With a charge concentration uniformly distributed over the thickness, the centroid of the package is located in its middle, and the electric field at $x = x_c$ is equal to the average value between the voltages at the front and rear of the package: $F_c = (F_f + F_r)/2$, defined as

$$F_c = \frac{V}{d} + \frac{en\delta}{\varepsilon \varepsilon_0} \left(\frac{x_c}{d} - \frac{1}{2} \right), \tag{8}$$

and F_c also grows as the package moves towards the charge collecting contact. The dependences of F_f , F_r and F_c on the corresponding coordinates are shown in Figure 7 for three

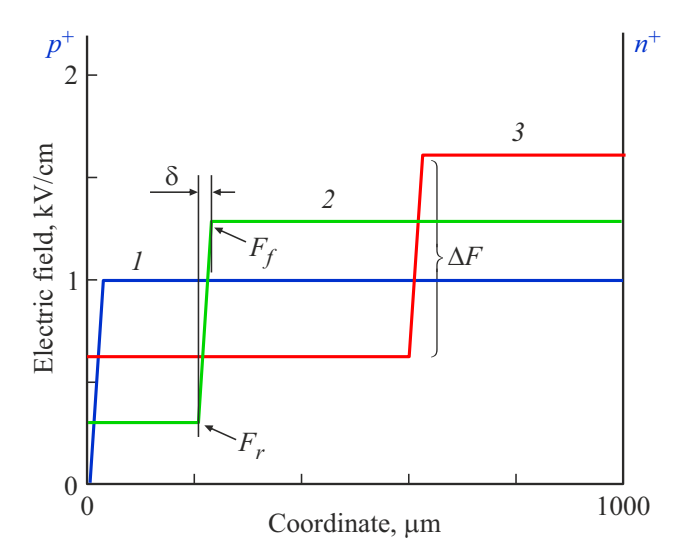


Figure 6. Illustration of electric field profiles in $p^+ - n - n^+$ -structure at V = 1 kV at three moments of electron drift: 1 - package separation from p^+ -contact at x = 0, 2 and 3 — package drift in the volume at x = 200 and $600 \, \mu\text{m}$, respectively.

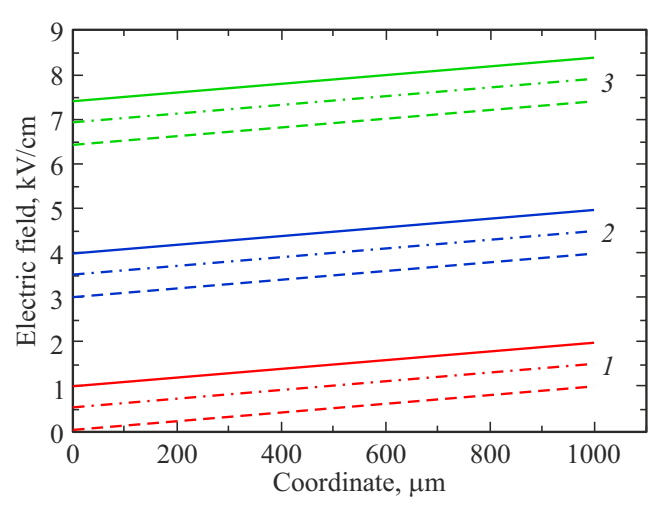


Figure 7. Dependences of F_f , F_r and F_c on the corresponding coordinates at voltages: 1 - 100, 2 - 400, 3 - 742 V. Designations of lines: solid $-F_f$, dashed $-F_r$, dashed-dotted $-F_c$.

values of V. It should be noted that F_c increases during the drift process for both packages with negative and positive charges, so the current in the responses should increase regardless of the type of drifting carriers, which is observed in the experiment.

Critical in the description of charge collection is the condition under which the process of electron drift passes from SCLC to drift controlled by the electric field of the package. According to Figure 1, for electrons it is realized at $V=100\,\mathrm{V}$, which determines the value of $\Delta F=1\,\mathrm{kV/cm}$. This jump gives a charge density equal to $1\cdot 10^{-9}\,\mathrm{C/cm^2}$, corresponding to the value $Q_{\rm col}$ obtained from $Q_{\rm col}(V)$ -dependence (Figure 3).

A similar analysis for the responses during hole collection shows that the prolonged pulse decay disappears at $V \approx 40\,\mathrm{V}$, which gives $\Delta F = 40\,\mathrm{V/cm}$ due to a lower concentration of NCC and, consequently, a lower charge being collected. In combination with the fact that in the pulses of holes, with a further increase in V, the tops of the pulses become close to flat, it can be concluded that the SCLC mode is practically not present when they are collected.

5. Conclusion

Analysis of current pulses generated in 1 mm thick Si p^+-n-n^+ -structure with electron and hole drift at 40 mK, showed that the charge collection process lasts $\sim 30\,\mathrm{ns}$ in the range of electric field of 200-300 V/cm, which is assumed when designing Si bolometric detectors with An estimate of internal thermal signal amplification. the time spent by NCC in the free state before their capture gives $\tau_{tr} \approx 370 \, \text{ns}$ for electrons and $> 1 \, \mu \text{s}$ for holes. Carrier trapping is highly likely attributable to the fact that shallow impurities become deep impurities at $T < 800 \,\mathrm{mK}$, the release of carriers from which becomes impossible during the collection time. Extrapolation of the obtained values t_{col} in relation to the operation of bolometric detectors with a thickness of units of centimeters indicates the possibility of limitations of their energy resolution.

It has been shown that two stages are observed in the process of NCC collection based on the space-charge-limited current mechanism and the drift of a thin carrier package controlled by the charge itself. For the latter, an analytical dependence of the characteristics of the electric field during drift was obtained, which made it possible to unambiguously explain the paradox of current growth at the top of pulses from both types of carriers.

It is important for the charge collection research methodology that the considered transformation of the electric field in the moving package and the sample as a whole should be taken into account when analyzing data obtained by the Transient Current Technique in the study of radiation degradation of detectors made of high-purity silicon. It is at the so-called point of inversion of the effective concentration $N_{\rm eff}$ sign that the conditions are realized under which the F(x)-profile determined from the shape of the pulse signals can be controlled not by the distribution of impurities, but by the effect of electric field disturbance by a drifting charge package.

With the target thickness of the bolometric detector of $\sim 3\,\mathrm{cm}$, the expected time for carrier collection is close to 1000 ns; moreover, to create an electric field of hundreds of V/cm, it will already be necessary to apply a voltage of $\sim 1000\,\mathrm{V}$ to the detector. Accordingly, the energy $\sim 10^3\,\mathrm{eV}$ will be released during the drift of each carriers created by antineutrino, i.e. $\sim 300\,\mathrm{times}$ greater than the energy of e-h-pairs formation in silicon, equal to

3.6 eV, which is valid only for $t_{\rm col} \ll \tau_{tr}$. The effect of internal amplification of the thermal signal will depend on the coordinate of the particle registration point in the sensitive element at $t_{\rm col}$ in hundreds of nanoseconds, which in turn will worsen the spectrometric characteristics of such detectors. Since τ_{tr} is proportional to σ^{-1} , where σ is the carrier capture cross-section for which data is not available at such low temperatures, continued experimentation is necessary due to the importance of the NCC lifetime for estimating the internal gain of Si bolometric detectors.

Funding

This study was conducted within the scientific program of the National Center for Physics and Mathematics, section No. 8. Stage 2023-2025.

Conflict of interest

The authors declare that they have no conflict of interest.

References

- [1] S. Cebrián. J. Phys.: Conf. Ser., 2502, 012004 (2023).DOI: 10.1088/1742-6596/2502/1/012004
- [2] M.F. Albakry, I. Alkhatib, D. Alonso-González, D.W.P. Amaral, J. Anczarski, T. Aralis, T. Aramaki, I.J. Arnquist, I.A. Langroudy, E. Azadbakht, C. Bathurst, R. Bhattacharyya, A.J. Biffl, P.L. Brink, M. Buchanan et al. Phys. Rev. D, 111, 012006 (2025). DOI: 10.1103/PhysRevD.111.012006
- [3] E. Armengaud, Q. Arnaud, C. Augier, A. Benoît, L. Bergé, J. Billard, A. Broniatowski, P. Camus, A. Cazes, M. Chapellier, F. Charlieux, M. De Jésus, L. Dumoulin, K. Eitel, J.-B. Filippini et al. Phys. Rev. D, 106, 062004 (2022). DOI: https://doi.org/10.1103/PhysRevD.106.062004
- [4] G. Beda, V.B. Brudanin, V.G. Egorov, D.V. Medvedev, V.S. Pogosov, M.V. Shirchenko, A.S. Starostin. Adv. High Energy Phys., 2012, 350150. DOI: 10.1155/2012/350150
- [5] A.A. Yukhimchuk, A.N. Golubkov, I.P. Maksimkin, I.L. Malikov, O.A. Moskalev, R.K. Musyaev, A.A. Seleznev, L.V. Grigorenko, V.N. Trofimov, A.S. Fomichev, A.V. Golubeva, V.N. Verbetsky, K.A. Kuzakov, S.V. Mitrokhin, A.I. Studenikin, A.P. Ivashkin, I.I. Tkachev. Fizmat, 1 (1), 5 (2023). (in Russian). DOI: 10.56304/S2949609823010057
- [6] Y. Giomataris, J.D. Vergados. Nucl. Instrum. Meth. A, 530, 330 (2004). https://doi.org/10.1016/j.nima.2004.04.223
- [7] B.S. Neganov, V.N. Trofimov. Sposob kalorimetricheskogo izmereniya ioniziruyushchikh izluchenii, USSR patent № 1037771 (in Russian).
- [8] E. Verbitskaya, V. Eremin, A. Zabrodskii, B. Dehning, C. Kurfurst, M. Sapinski, M.R. Bartosik, N. Egorov, J. Harkonen. Nucl. Instrum. Meth. A, 796, 118 (2015). http://dx.doi.org/10.1016/j.nima.2015.03.027
- [9] V. Eremin, A. Shepelev, E. Verbitskaya. JINST, 17, P11037 (2022). DOI: 10.1088/1748-0221/17/11/P11037

- [10] E.M. Verbitskaya, I.V. Eremin, A.A. Podoskin, V.O. Zbrozhek, S.O. Slipchenko, N.N. Fadeeva, A.A. Yablokov, V.K. Eremin. FTP 58, 415 (2024). (in Russian).
 DOI: 10.61011/FTP.2024.08.59200.7067
 [E.M. Verbitskaya, I.V. Eremin, A.A. Podoskin, V.O. Zbrozhek, S.O. Slipchenko, N.N. Fadeeva, A.A. Yablokov, V.K. Eremin. Semiconductors, 58, 381 (2024). https://doi.org/10.61011/SC.2024.08.59888.7067
- [11] S. Ramo. Proc. IRE, 27, 584 (1939).
- [12] V. Eremin, A. Shepelev, E. Verbitskaya, C. Zamantzas, A. Galkin. J. Appl. Phys., 123, 204501 (2018). https://doi.org/10.1063/1.5029533
- [13] G. Kramberger, V. Cindro, I. Mandíc, M. Mikuź, M. Zavrtanik. Nucl. Instrum. Meth. A, 481, 297 (2002).
- [14] C. Canali, G. Ottaviani, A. Taroni. Solid-State Electron., 14, 661 (1971).
- [15] P.A. Tove, L.G. Anderson. Solid-State Electron., **16**, 961 (1973).

Translated by A.Akhtyamov